CHEMICAL ENGINEERING TRANSACTIONS

VOL. 47, 2016

A publication of
AIDIC
The Italian Association
of Chemical Engineering
Online at www.aidic.it/cet

Guest Editors: Angelo Chianese, Luca Di Palma, Elisabetta Petrucci, Marco Stoller

ISBN 978-88-95608-38-9; **ISSN** 2283-9216

DOI: 10.3303/CET1647018

Synthesis and Characterization of Magnetic Nanocomposites for Environmental Remediation

Habiba Shirinova[a], Luca Di Palma*[b], Fabrizio Sarasini[b], Jacopo Tirillò[b], Mahammadali A. Ramazanov [a], Flora Hajiyeva[a], Diana Sannino[c], Massimiliano Polichetti[d], Armando Galluzzi[d]

[a]Baku State University, Physics Faculty, Z. Khalilov Street, 23 Baku, AZ1148, Azerbaijan
[b]Sapienza University, Department of Chemical Engineering Materials Environment, Via Eudossiana 18, 00184, Roma - INSTM, UdR Uniroma1 Sapienza
[c]Department Industrial Engineering, University of Salerno, via Giovanni Paolo II, 132-Fisciano (SA)-84084-Italy
[d]Department of Physics "E.R. Caianiello", University of Salerno, via Giovanni Paolo II, 132-Fisciano (SA)-84084-Italy
luca.dipalma@uniroma1.it

In the present study, the effect of nano-magnetite (Fe_3O_4) content on mechanical and magnetic properties of polypropylene matrix is investigated. Magnetite nanoparticles were successfully synthesized by co-precipitation while the composites were prepared by an ex situ processing method involving solvent casting followed by compression molding. The nanoparticles and resulting nanocomposites were characterized by X-ray diffraction, thermogravimetric analysis, scanning electron microscopy, tensile testing and vibrating sample magnetometry. It was found that composites have tailorable mechanical and magnetic properties dependent on the content of magnetic filler. Increase of concentration of magnetite particles provides a significant increase of Young's modulus without affecting the yield strength and the ductility. As regards the magnetic properties, nanocomposites having 10 wt% of nanoparticles exhibited a superparamagnetic behaviour that can be exploited in environmental applications.

1. Introduction

Among the broad spectrum of nanoscale materials being investigated for various environmental and biomedical applications, magnetic nanoparticles (MNPs) have gained significant attention due to their interesting magnetic properties, which make them of great interest to researchers in magnetic fluids, catalysis, biotechnology/biomedicine, magnetic resonance imaging, data storage, and environmental remediation (Zhu et al., 2013). This class of nanomaterials includes metallic and bimetallic nanoparticles, metal oxides, ferrites, and superparamagnetic iron oxide nanoparticles (Huber, 2005; Maicas et al., 2010; Cornell and Schwertmann, 2003; Mathew and Juang, 2007; Sarno et al., 2015;). While a number of suitable methods have been developed for their synthesis, successful application of such magnetic nanoparticles in the areas listed above is highly dependent on the stability of the particles under a range of different conditions and, in most of the envisaged applications, the particles perform best when the size of the nanoparticles is below a critical value, which is dependent on the material but is typically around 10–20 nm. Targeting to various applications, efforts have been made to disperse the MNPs in a matrix, e.g., to prevent superparamagnetic NPs from aggregating into large ferromagnetic species. In general it is very difficult to prepare complex structures for specific high-tech applications with pure nanopowders. A recently active concept for improving the flexibility and processability is based on the hybridization of ceramic materials with organic polymers (Kalia et al., 2014; Horst et al., 2015; Reinholds et al., 2012; Tsonos et al., 2015; Che et al., 2015). Magnetic polymer nanocomposites can be defined as materials composed of an inorganic magnetic component in the form of particles, fibers or lamellae with at least one dimension in the nanometer range embedded in an organic polymer. The benefits of nanocomposites are to integrate several component materials and their properties in a single material. In magnetic polymer nanocomposites, organic–inorganic synergies add new properties that cannot be achieved in either single organic or individual inorganic components. The final properties of these

Please cite this article as: Shirinova H., Di Palma L., Sarasini F., Tirillo J., Ramazanov M., Hajiyeva F., Sannino D., Polichetti M., Galluzzi A., 2016, Synthesis and characterization of magnetic nanocomposites for environmental remediation, Chemical Engineering Transactions, 47, 103-108 DOI: 10.3303/CET1647018

nanocomposites mainly depend on parameters such as filler size, method of preparation and the dispersion of nanoparticles into the polymer matrix (Ishida et al., 2000). Among the nanosized fillers, iron oxides have attracted significant interest and especially magnetite (Fe_3O_4) and maghemite (γ-Fe_2O_3), have found numerous potential applications in magnetic recording technology, pigments, catalysis, photocatalysis, medical uses and environmental processes. This can be ascribed to their magnetic properties, biocompatibility, biodegradability and low cost. In this framework the objective of this study was to develop magnetite–polymer based nanocomposites possessing magnetic properties together with structural flexibility that would be valuable for the manufacture of complex structures or coatings to be used in the field of environmental remediation, in particular for heavy metals removal from water. In particular, magnetite (Fe_3O_4) as the magnetic nanoparticles and polypropylene (PP) as the polymer matrix were used.

2. Materials and Methods

2.1 Materials

The chemical used were ferrous sulphate heptahydrate ($FeSO_4 \cdot 7H_2O$, 98% chemically pure), ferric chloride hexahydrate ($FeCl_3 \cdot 6H_2O$, 98% chemically pure), ammonium hydroxide [25% (by mass) NH_3 in water], polyethylene glycol 6000 (PEG6000), toluene and deionized water.

2.2 Synthesis of magnetite nanoparticles

Co-precipitation is a facile and convenient way to synthesize MNPs (metal oxides and ferrites) from aqueous salt solutions by the addition of a base under inert atmosphere at room temperature or at elevated temperature. Nanoparticles of Fe_3O_4 were synthesized by hydrolysis of an aqueous solution containing iron salts and a base at room temperature in ambient atmosphere. Fe_3O_4 magnetic nanoparticles were prepared on the basis of co-precipitation Fe^{2+} and Fe^{3+} with a molar ratio of 3:2. In this study, instead of a stabilizing agent, polyethylene glycol was used. As the precipitating agent under a nitrogen atmosphere ammonium hydroxide (NH_4OH) was added. Salts $FeSO_4 \times 7H_2O$ and $FeCl_3 \times 6H_2O$ were dissolved in 100 ml-bidistilled water. The mixture was stirred vigorously using a magnetic stirrer at 80°C. For 100 ml solution of salts 0.5 g of polyethylene glycol with molecular weight of 6000 were added. The surfactant lowers the surface tension at the interface between materials and modulates the available surface energy of the particles so that the surface tension decreases, allowing more particles to escape the aggregation process and generally lowering the mean particle size. It is well known that $Fe(OH)_2$ and $Fe(OH)_3$ formed at pH>8 by the hydroxylation of the ferrous and ferric ions under anaerobic conditions. To achieve an optimum pH equal to 11, in 100 ml of Fe^{3+} and Fe^{2+} in a molar ratio of 3:2 containing 0.5 g of polyethylene glycol was added in a fast stream 100 ml of 25% ammonium hydroxide. When ammonium hydroxide was added, a precipitate was immediately produced. Consequently, the formation of Fe_3O_4 MNPs occurred with black precipitation. The possible reaction for the formation of Fe_3O_4 MNPs is as follows:

$Fe^{3+} + 3OH^- \rightarrow Fe(OH)_3$

$Fe(OH)_3 \rightarrow FeOOH + H_2O$

$Fe^{2+} + 2OH^- \rightarrow Fe(OH)_2$

$$2FeOOH + Fe(OH)_2 \rightarrow Fe_3O_4\downarrow + 2H_2O \quad (1)$$

The mixture was stirred for an additional 1 hour. The reaction is fast, with a high yielding and magnetite crystals are seen instantaneously after addition of the iron source. It is essential that the whole reacting mixture be free of oxygen, otherwise magnetite can be oxidised to γ-Fe_2O_3 in the reaction medium. The pH value of the filtrate was 11.1–11.3. The precipitate was washed with bidistilled water six times to remove excess of ammonium ions. Finally, the humid suspension was evaporated and dried for 24 hours. After the drying process, magnetic iron oxide (Fe_3O_4) nanocrystals were ground. The factors that influence the stability, size and monodispersity of the nanoparticles include temperature, pH , the nature of the precipitant, the ratio of the components, the nature of the surfactant, the surfactant concentration.

2.3 Synthesis of magnetic polymer nanocomposites

Composites were prepared with different amounts of magnetite nanoparticles, namely 1%, 5%, 8%, 10% by weight. 0.5 g of PP were dissolved in an organic solvent (80 ml of toluene) at temperature of 120 °C for 25-30 min. After complete dissolution of the polymer in toluene, a relatively high content (up to 10%) of iron oxide (Fe_3O_4) nanofiller was added without cooling the polymer solution and this solution was mixed in a magnetic stirrer for 2 hours. After mixing, solution was poured in petri dishes and allowed to evaporate in vacuum over 24 hours. Nanocomposite samples were prepared from this final material by hot pressing method at the melting temperature of PP and with a pressure of 10 MPa, for 4 min and rapidly cooled with water with rate β=20 deg/min.

2.4 Characterization techniques

The crystalline structure of magnetite nanoparticles was characterized by X-ray diffraction (XRD, Philips X-PERT). A step–scan mode was used in the 2θ range from 20° to 70° with a step width of 0.01° and a counting time of 7 s per step. The used radiation was monochromated CuKα (40 kV – 40 mA). The thermal stability of nanoparticles was evaluated using thermogravimetric analyser (Setsys evolution TGA/DSC). Analysed samples were heated from 120°C to 800°C at a heating rate of 10°C/min under a nitrogen flow of 30 mL/min.

The specimens for the mechanical characterization were cut from the disks according to the geometry and dimensions (Figure 1).

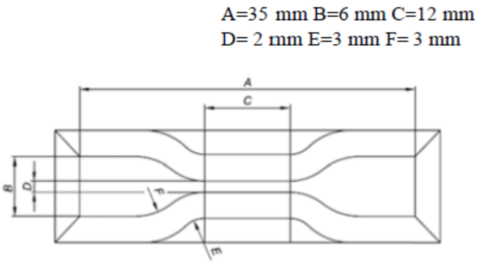

Figure 1: Geometry and dimensions of the tensile specimen die

The tensile tests were carried out in displacement control (cross-head speed = 10 mm/min) on a Zwick/Roell Z010 universal testing machine equipped with a 1 kN load cell.

The morphology of nanoparticles and of the fracture surfaces of nanocomposites was investigated using a field emission scanning electron microscope (Zeiss, Auriga). All specimens were sputter coated with chromium prior to examination.

DC magnetic measurements were performed by a Vibrating Sample Magnetometer (VSM) on three different materials, namely neat PP and PP loaded with 5 wt%, 8 wt% and 10 wt% of nanoparticles. The m(T) measurements of magnetic moment as a function of temperature were performed in Zero Field Cooling (ZFC)-Field Cooling (FC) conditions. More precisely, the sample was first cooled down to 5 K in absence of field, then the field was switched on at 0.1 Tesla and the data were acquired for increasing temperature (ZFC) up to room temperature (300 K). After that, the sample was cooled down again and FC magnetic moment was acquired in presence of the field. For the m(H) measurements of the magnetic moment as a function of magnetic field, the sample was first thermally stabilized to the measurement temperature in absence of field. Then, the field was ramped with a sweep rate of $1 \cdot 10^{-2}$ T/s to reach +9 T, then back to -9 T, and finally to +9 T again in order to acquire the complete m(H) loop.

3. Results and Discussion

XRD is an effective characterization technique to confirm the crystal structure of the synthesized magnetite nanoparticles. The XRD spectrum for magnetite nanoparticles is shown in Figure 2. All diffraction peaks in Figure 2 are consistent with the standard cubic structure of magnetite (JCPDS card No. 79-0418) (Shen et al., 2014; Zhao et al., 2006). Typical scanning electron micrographs of the nanoparticles are shown in Figure 3 at different magnifications. Most of the nanoparticles appeared to be of irregular spherical shape with diameters in the 10-20 nm range. It is also possible to note a significant level of agglomeration. The TGA thermogram of magnetite nanoparticles is shown in Figure 4. The TGA curve shows a high thermal stability with a weight loss over the temperature range from 120 °C to 800 °C of about 2% that might be due to the loss of the remaining water and synthesis agents (Shen et al., 2014).

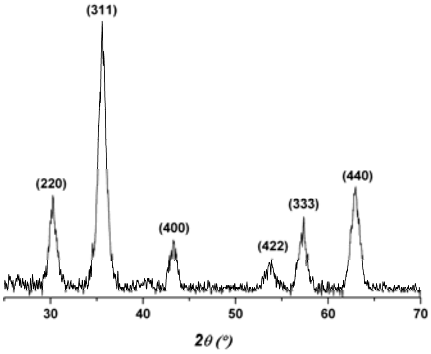

Figure 2: XRD pattern of Fe_3O_4 nanoparticles

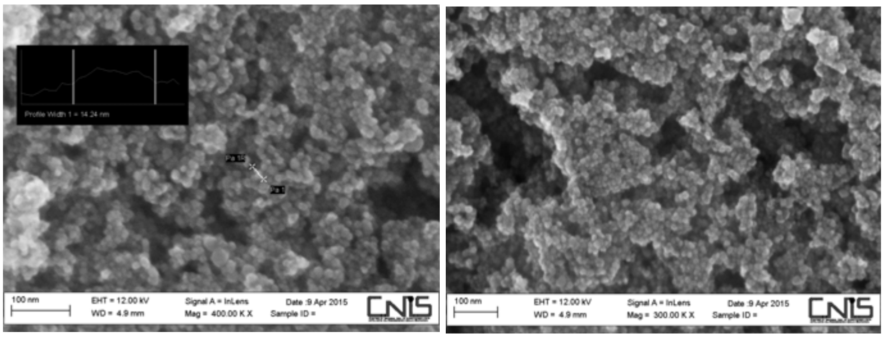

Figure 3: FE-SEM micrographs of Fe_3O_4 nanoparticles

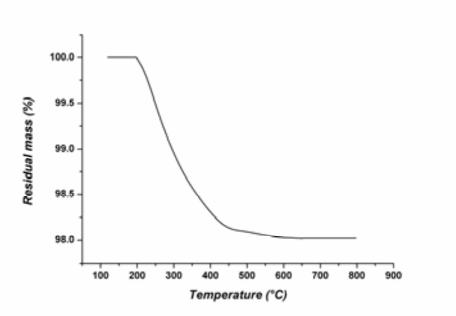

Figure 4: TGA curve of magnetite nanoparticles

The tensile properties of PP-based nanocomposites are summarized in Table 1. The addition of magnetite nanoparticles caused an increase in Young's modulus with increasing content and an almost constant value of yield strength. It is to be noted that even at the highest amount of nanoparticles, the specimens exhibited a ductile behavior with extensive plastic deformation. The results do not show clear trends as regards the mechanical properties, in particular for the elongation at break, due to the presence of a non-homogeneous and uniform dispersion of the nanofillers within the matrix that can significantly affect the mechanical behavior.

Table 1: Summary of tensile properties of PP-based nanocomposites

Specimen	Yield strength (MPa)	Young's modulus (MPa)	Strain at break (%)
PP_1wt% Fe_3O_4	16.78 ± 1.37	848.10 ± 52.00	281.04 ± 30.52
PP_5wt% Fe_3O_4	19.01 ± 0.19	883.70 ± 29.48	322.14 ± 22.81
PP_8wt% Fe_3O_4	18.37 ± 1.85	1075.80 ± 18.63	191.05 ± 61.37
PP_10wt% Fe_3O_4	20.77 ± 1.18	1092.90 ± 53.09	402.50 ± 6.99

Concerning the magnetic properties, m(T) measurements of the magnetic moment *m* as function of the temperature *T* have been performed on neat PP films and on the samples filled with 5%, 8% and 10 wt% of Fe_3O_4 nanoparticles. The m(T) at 0.1 Tesla on neat PP sample (not reported) showed for T ≥ 60K a linear diamagnetic behavior with temperature. For T ≤ 60K two magnetic transitions were detected: the first at T ≈ 60 K and the second one at T ≈ 20 K. The m(T) curves for 5 wt% and 10 wt% filled samples are reported in Figure 5.

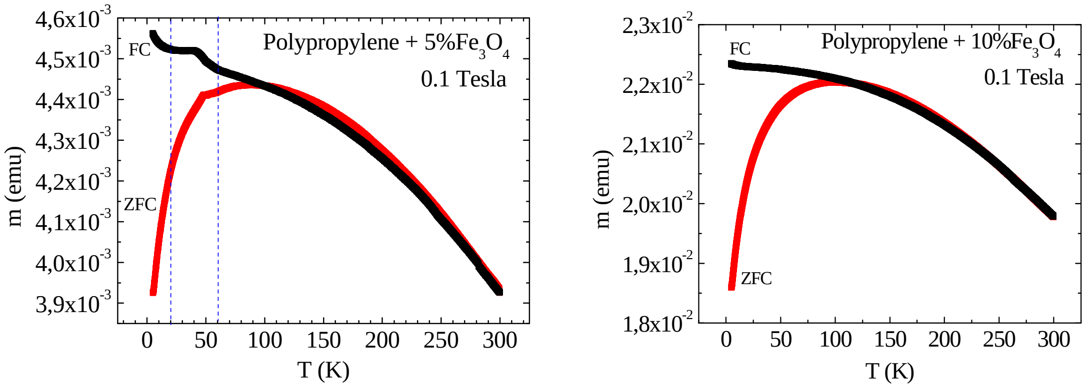

Figure 5: ZFC and FC curves of m(T) at 0.1 Tesla on PP-based nanocomposite films loaded with 5 wt% (left) and with 10 wt% (right) of Fe_3O_4 nanoparticles

In PP film filled with 5 wt% of Fe_3O_4 nanoparticles, for 20 K < T < 60 K a magnetic transition is visible both in the Zero Field Cooling (ZFC) and Field Cooling (FC) curves of m(T), likely due to the PP. Nevertheless, it is possible to observe a positive magnetic moment, the presence of a peak in the ZFC curve and also a region of reversibility between the ZFC and FC curves. These properties in the m(T) curve suggest a superparamagnetic (SPM) behavior of the sample with a blocking temperature (TB) of about 90 K. In the PP_10wt% Fe_3O_4 sample (Figure 5, right), the magnetic transition at low temperature is no more visible since the signal is stronger than the PP_5wt% Fe_3O_4. Nevertheless, the same total SPM behavior in m(T) as for the PP_5wt% Fe_3O_4 sample is reported with TB of about 100 K. The m(H) curve measured at T=300K on neat PP sample revealed a clear diamagnetic behavior, consistent with its m(T) curve. This explains also the negative slope of the m(H) dependence at high magnetic field measured at T=300K on PP film filled with 5 wt% of Fe_3O_4 nanoparticles and reported in Figure 6 (left). However, the whole m(H) curve of PP_5wt% Fe_3O_4 sample is coherent with a SPM behavior of this material. This behavior is even more evident in the measurement on the PP_10wt% Fe_3O_4 sample, reported in Figure 6 (right) where the diamagnetic contribution coming from the PP is totally dominated by the magnetic signal coming from the nanoparticles. The insets of both left and right panels of Figure 6 show a small hysteresis close to H=0 which is within the error coming from the presence of the residual field in the superconducting magnet used for the experiments.

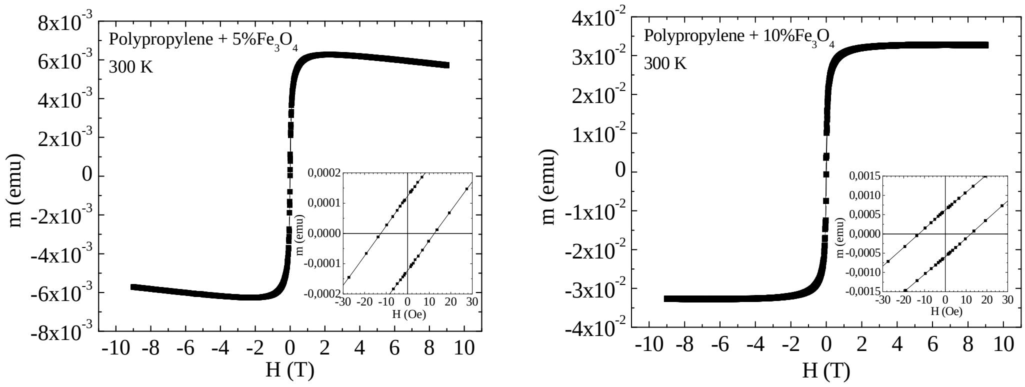

Figure 6: m(H) at 300K on PP-based nanocomposite films loaded with 5 wt% (left) and 10 wt% (right) of Fe_3O_4 nanoparticles

It is worth underlining that for the PP_5wt% Fe_3O_4 the maximum value of the magnetic moment H (m_{sat}) is detected at a magnetic field around 2.2 Tesla, although the 90% of the maximum magnetic moment is already reached at a field H (90% m_{max}) of about 0.5 Tesla. An analogous behavior is reported also for the other measured samples. All the characteristics extracted from the magnetic measurements are outlined in Table 2.

Table 2: Magnetic features of the samples

Samples	H (90% m_{max}) (T)	H (m_{sat}) (T)	T_B (K)
PP_5wt% Fe_3O_4	0.5	2.2	90
PP_8wt% Fe_3O_4	0.7	6.5	135
PP_10wt% Fe_3O_4	0.65	6.5	100

4. Conclusions

This work reported the preliminary results on the synthesis and characterization on magnetic polymer nanocomposites. Magnetite nanoparticles were synthesized by co-precipitation whilst nanocomposites were manufactured by an ex situ processing method involving solvent casting followed by compression molding. The method of preparation of the composites reported here is relatively simple and the results show that both mechanical and magnetic properties can be tailored by the judicious choice of compositions. As the materials investigated exhibited structural flexibility and magnetic properties, these composites show the potential of being used in complex applications, including those related to the environmental remediation. In particular, the performed magnetic measurements show that the samples with a percentage of Fe_3O_4 nanoparticles equal or higher than 5% appear attractive for the applications, also because the magnetic properties due to the presence of the magnetite nanoparticles can already be exploited at reasonable low field such as 0.5 Tesla.

References

Che H.X., Gwee S.J., Ahmad A.L., Lim J., 2015, Guided Assembly of Magnetic Nanocomposite with Open Shell Structure for Water Remediation, Chemical Engineering Transactions, 45, 1489-1494.

Cornell R.M., Schwertmann U., Eds., 2003, The iron oxides: structure, properties, reactions, occurrences and uses. Wiley-VCH Verlag GmbH & Co, Weinheim, Germany.

Horst M.F., Alvarez M., Lassalle V.L., 2015, Removal of heavy metals from wastewater using magnetic nanocomposites: Analysis of the experimental conditions, Separation Science and Technology, DOI: 10.1080/01496395.2015.1086801.

Huber D.L., 2005, Synthesis, properties, and applications of iron nanoparticles, Small, 1, 482-501.

Ishida H., Campbell S., Blackwell J., 2000, General approach to nanocomposite preparation, Chemistry of Materials, 12, 1260–1267.

Kalia S., Kango S., Kumar A., Haldorai Y., Kumari B., Kumar R., 2014, Magnetic polymer nanocomposites for environmental and biomedical applications, Colloid and Polymer Science, 292, 2025-2052.

Maicas M., Sanz M., Cui H., Aroca C., Sanchez P., 2010, Magnetic properties and morphology of Ni nanoparticles synthesized in gas phase, Journal of Magnetism and Magnetic Materials, 322, 3485-3489.

Mathew D.S., Juang R.S., 2007, An overview of the structure and magnetism of spinel ferrite nanoparticles and their synthesis in microemulsions, Chemical Engineering Journal, 129, 51-65.

Reinholds I., Kalkis V., Zicans J., Merijs Meri R., Grigalovica A., Maiorov M., 2012, Mechanical, structural and magnetic properties of polypropylene/iron ferrite magnetic nanocomposites, IOP Conf. Series: Materials Science and Engineering, 38, 012030.

Sarno M., Cirillo C., Ciambelli P., 2015, Fluorescent and Magnetic Monodisperse Fe_3O_4 Nanoparticles, Chemical Engineering Transactions, 43, 691-696.

Shen M., Yu Y., Fan G., Chen G., Jin Y.M., Tang W., Jia W., 2014, The synthesis and characterization of monodispersed chitosan-coated Fe_3O_4 nanoparticles via a facile one-step solvothermal process for adsorption of bovine serum albumin, Nanoscale Research Letters, 9, 296.

Tsonos C., Pandis C., Soin N., Sakellari D., Myrovali E., Kripotou S., Kanapitsas A., Siores E., 2015, Multifunctional nanocomposites of poly(vinylidene fluoride) reinforced by carbon nanotubes and magnetite nanoparticles, eXPRESS Polymer Letters, 9, 1104–1118.

Zhao S.-Y., Lee D.K., Kim C.W., Cha H.G., Kim Y.H., Kang Y.S., 2006, Synthesis of magnetic nanoparticles of Fe_3O_4 and $CoFe_2O_4$ and their surface modification by surfactant adsorption, Bulletin of the Korean Chemical Society, 27, 237-242.

Zhu J., Wei S., Chen M., Gu H., Rapole S.B., Pallavkar S., Ho T.C., Hopper J., Guo Z., 2013, Magnetic nanocomposites for environmental remediation, Advanced Powder Technology, 24, 459-467.